

Heat Shock Protein (HSP) 72 Enters Early Endosomes Preparatory to Cell Release

Punit Kaur^{1,2*} and Alexander Asea³

¹Department of Microbiology, Biochemistry and Immunology, Morehouse School of Medicine, 720 Westview Drive SW, Atlanta, GA 30310, USA

²Department of Experimental Radiation Oncology, University of Texas MD Anderson Cancer Center, 1515 Holcombe Boulevard, Houston, Texas 77030, USA

³Department of Neuroscience Research and Deanship for Scientific Research, University of Dammam, Dammam Khobar Coastal Road, Dammam 33441, Saudi Arabia

Abstract

Purpose: To establish the mechanism by which hyperthermia induces the release of Hsp72 in tumor specific peptides for delivery to antigen presenting cells (APC).

Materials and methods: 4T1 scrb-shRNA^{GFP} and Hsp72-shRNA^{GFP} cells were injected into the breast pad of a female BALB/c mouse for temperature kinetics of mice exposed to HT using circulating water bath set and nanoshell-mediated hyperthermia. Baseline and heat-induced intracellular Hsp72 expression was measured by immunoblotting with anti-Hsp72. Four hours post hyperthermia (HT) treatment Hsp72 colocalization was determined using inhibitors and exosomes were recovered from the supernatant and Hsp72 levels were measured. Tumor size was measured after hyperthermia.

Results: In this study, we show that the released Hsp72 is found in two forms: 1) within highly immunologically-active exosomes, known to be enriched in major histocompatibility complex (MHC) class I and II complexes, co-stimulatory molecules (CD40, CD80, CD86) and specifically members of the HSP70 family (including Hsp72, Hsp73, Hsp75, Grp78) and HSP90 family (including Hsp82, Hsp90, Grp96, Grp98) and, 2) as Hsp72-PC, in which free Hsp72 is chaperoning tumor specific peptides. Further, we show that exposure of 4T1-bearing tumors to hyperthermia (41°C, 60 min) induces significant tumor regression ($p < 0.05$) as compared to 4T1-bearing mice maintained at ambient temperature (25°C, 60 min) tumor. However, repeated injection of 4T1 tumor-bearing mice with anti-Hsp72 antibody, abrogated hyperthermia-induced tumor regression. Blood samples taken at various times confirmed that the blocking antibody significantly reduced plasma Hsp72 levels.

Conclusions: Our results suggested that hyperthermia stimulated tumor regression, in part, by stimulating the release of Hsp72 from tumors which is taken up by APC preparatory to activating CD8⁺ CTL cytotoxic responses against tumors. Since HSP are found in all cellular organisms, it is likely be applicable to the prevention/treatment of diseases of agriculturally relevant animals. It is expected to contribute to the broader understanding of intracellular trafficking pathways as an approach to therapy.

Keywords: Endosomes; Hsp72; Hyperthermia; Rab proteins; Thermal therapy; Tumors

Abbreviations: APC: Antigen Presenting Cells; CTL: Cytotoxic T Lymphocytes; EE: Early Endosome; HSP: Heat Shock Proteins; HT: Hyperthermia; LE: Late Endosomes; MHC: Major Histocompatibility Complex; RE: Recycling Endosomes; TAA: Tumor-Associated Antigens

Introduction

Hyperthermia (HT) as an effective intervention strategy has increasingly become a potentially attractive approach to treating cancer because of its ability to promote the production of therapeutically beneficial, tumor-derived, heat shock proteins (HSP) [1]. In *in vitro* experiments, we and others have demonstrated that HSP released in response to exposure to HT, the inducible Hsp72, functions both as a chaperone by binding tumor-associated antigens (TAA) for delivery to antigen presenting cells (APC) [2], which respond by releasing pro-inflammatory cytokines [3,4], chemokine and nitric oxide and as a cytokine itself [5]. This dual function of released Hsp72 is called the chaperokine activity [6].

HT induces the release of Hsp72 by a yet unknown intracellular trafficking pathway which is independent of the classical protein transport pathway utilized by most proteins released from cells [7,8]. We have shown that the released Hsp72 is found in two forms: 1) within highly immunologically-active exosomes, known to be enriched in major histocompatibility complex (MHC) class I and II complexes, co-

stimulatory molecules (CD40, CD80, CD86) and specifically members of the HSP70 family (including Hsp72, Hsp73, Hsp75, Grp78) and HSP90 family (including Hsp82, Hsp90, Grp96, Grp98) and, 2) as Hsp72-PC, in which free Hsp72 is chaperoning tumor specific peptide [8]. Although HT-induced Hsp72 released by tumors has been demonstrated to promote the generation of immune responses against tumor-associated antigens, relatively little is known about the intracellular trafficking pathway utilized by Hsp72 to gain access to the extracellular milieu or the mechanism(s) by which released Hsp72 stimulates anti-tumor responses. Hsp72 functions to specifically chaperone tumor-associated antigens (TAA). When taken up by APC,

***Corresponding author:** Kaur P, Department of Microbiology, Biochemistry and Immunology, Morehouse School of Medicine, 720 Westview Drive SW, Atlanta, GA 30310 and Department of Experimental Radiation Oncology, University of Texas MD Anderson Cancer Center, 1515 Holcombe Boulevard, Houston, Texas 77030, USA, Tel: +1(404)756-5795; Fax: +1(404)752-1179; Email: pkaur@msm.edu, pkaur@mdanderson.org

Received: September 08, 2016; **Accepted:** October 27, 2016; **Published:** October 28, 2016

Citation: Kaur P, Asea A (2016) Heat Shock Protein (HSP) 72 Enters Early Endosomes Preparatory to Cell Release. J Cell Sci Ther 7: 253. doi: [10.4172/2157-7013.1000253](https://doi.org/10.4172/2157-7013.1000253)

Copyright: © 2016 Kaur P, et al. This is an open-access article distributed under the terms of the Creative Commons Attribution License, which permits unrestricted use, distribution, and reproduction in any medium, provided the original author and source are credited.

TAA are presented in association with MHC class I to CD8 positive T cells for the generation of cytotoxic T lymphocytes (CTL) directed against tumor cells bearing the specific TAA. Hsp72 trafficking occurs via the endocytic pathway and that there is a fundamental difference in the compositional characteristics of hyperthermia- or radiotherapy-induced Hsp72. We have also shown that TAA, specifically HER2, when transfected into tumor cells, leads to the generation of CTL directed against tumor cells bearing the specific TAA (HER2); and that unique peptide sequences in the TAA (HER2) can be found within released Hsp72-containing exosomes. It is important to understand the mechanism by which hyperthermia stimulates tumor killing, so that it will become possible to translate these findings to design molecular targets to enhance the production and release of tumor-derived HSP in response to hyperthermia.

Material and Methods

Cells and culture conditions

4T1 is a highly metastatic breast cancer cell line derived from a spontaneously arising BALB/c mammary tumor was purchased from ATCC collection. When injected into the abdominal breast gland of female BALB/c mice (8-12 weeks old), 4T1 spontaneously produces highly metastatic tumors that can metastasize to the lung, liver, lymph nodes and brain while the primary tumor is growing in situ. The primary tumor does not have to be removed to induce metastatic growth. The tumor growth and metastatic spread of 4T1 cells in BALB/c mice very closely mimic human breast cancer. 4T1 cells were maintained on Dubelcco's modified Eagle media (Invitrogen, Carlsbad, CA) containing 2 mM L-glutamine and adjusted to contain 1.5 g/L sodium bicarbonate, 4.5 g/L glucose, 10 mM HEPES, and 1.0 mM sodium pyruvate, and 10% fetal bovine serum Penicillin (100 units/ml) and streptomycin (100 mg/ml). at 37°C in a humidified incubator with 5% CO₂ atmosphere.

Animals

Female 6-8 weeks old BALB/c mice purchased from Charles River Laboratories (Wilmington, MA) were housed under pathogen-free conditions and were used throughout these studies. The studies have been reviewed and approved by the institutional animal care and use committee (IACUC) at Morehouse School of Medicine (Atlanta, GA) and MD Anderson Cancer Center (Houston, TX).

Thermometry

We next optimized experimental conditions required for the effective monitoring of HT treatment-induced release of GFP-tagged Hsp72 from tumors. Figure 1a illustrates the setup used when mice are exposed to HT. A thermistor rectal probe can be seen inserted into the rectum (arrow A), and is used to monitor core temperature. A second probe, a hypodermic needle microprobe is inserted into the tumor and is used to monitor tumor temperature. The tip of the probe can be seen inside the tumor (arrow B2), while the rest of the probe is seen on the mouse's thigh (arrow B1). The GFP-tagged tumor is shown in green (arrow C) (Figure 1a). An additional probe is placed into the water bath, and is used to monitor water temperature. All probes are connected to a 7-channel type T thermocouple input which automatically monitors room temperature acquisition and analysis software (Physitemp, Clifton, NJ). The lightly anesthetized mouse is then placed into a Styrofoam box with an area cutout which only exposes the tumor to the circulating water bath.

Immunoblotting

Following various treatment protocols, cells were lysed using RIPA

buffer containing appropriate protease inhibitor cocktail and the protein concentration was determined using the Bradford method (Bio-Rad, Hercules, CA) using a DU-650 Spectrophotometer (Beckman Coulter). Total cell extracts (50 µg) were run in a 12 % SDS-PAGE gel and transferred onto a nitrocellulose membrane. Membrane was blocked for 1 h at 4°C with TTBS (Tween 20 -Tris buffered saline) containing 5% milk. After rinse, the membrane was probed with a primary antibody against Hsp70 in a dilution ratio of 1:2000 (StressGen Biotechnologies). Antibodies were diluted in T-TBS containing 5% milk. After 1 h incubation at room temperature, the membrane was washed in T-TBS three times. HRP-conjugated IgG corresponding secondary antibodies (Sigma-Aldrich, St. Louis, Missouri), were added and membrane incubated for 30 minutes at room temperature. After additional washes, bands were visualized using enhanced chemiluminescence (Amersham, Little Chalfont, UK). Protein loading control was used as β-actin (Abcam). Appropriate secondary antibodies (Santa Cruz, and Sigma) were used in the study.

Fluorescence microscopy

Standard fluorescence microscopy was performed using an Olympus CKX41 microscope. DP71 CCD camera was used to capture phase contrast and GFP fluorescence images with DP71 image acquisition interface software (Olympus).

Live animal imaging

4T1-controlshRNA and 4T1-Hsp72 shRNA cells (1×10^4) were injected into mammary pad of female BALB/c mice. The mice were anesthetized approximately 5 minutes using Isoflurane gas before imaging and placed inside the imaging system. BALB/c mice hair also emit auto fluorescence; the hair was removed by shaving. On the indicated days, spectral fluorescence images were captured using the Maestro™ *in vivo* imaging system (CRI, Inc., Woburn, MA). An excitation band pass filter from 445 nm to 490 nm and an emission filter over 515 nm were used in the study. The tunable filter was automatically spaced in 10 nm increments from 500 nm to 720 nm while the camera captured fluorescence images at each wavelength with constant exposure. RGB (red-green-blue) color fluorescence images were synthesized from the spectral cube by mapping the spectral data into those color channels. All the fluorescence images obtained as RGB images in the present study were derived from the spectral datasets. Spectral unmixing was done to segregate skin and hair auto fluorescence and to measure the true GFP signal.

Animals and tumor challenges

BALB/c mice were challenged in the abdominal mammary gland and tumor volume measured at regular intervals using an electronic caliper until tumor size reached 1,000 mm³. The tumor volume was estimated using a formula of an ellipsoid (length × width × height × 0.5236). All animals were treated humanely and in accordance with the guidelines of the committee on the care and use of laboratory animals of the institute of animal resources, national research council and Morehouse School of Medicine.

Enzyme linked immunosorbant assay (ELISA)

Following various treatment protocols, either human serum or cell culture medium was centrifuged to discard floating cells and cellular debris and the total protein content was determined by Bradford analysis using bovine serum albumin as a standard. The supernatant was aliquoted and treated with Asea-0821 buffer (containing 1% Triton X-100+1% Lubrol WX+0.5% Brij 98 in 1X PBS) for 30 min at 4°C with

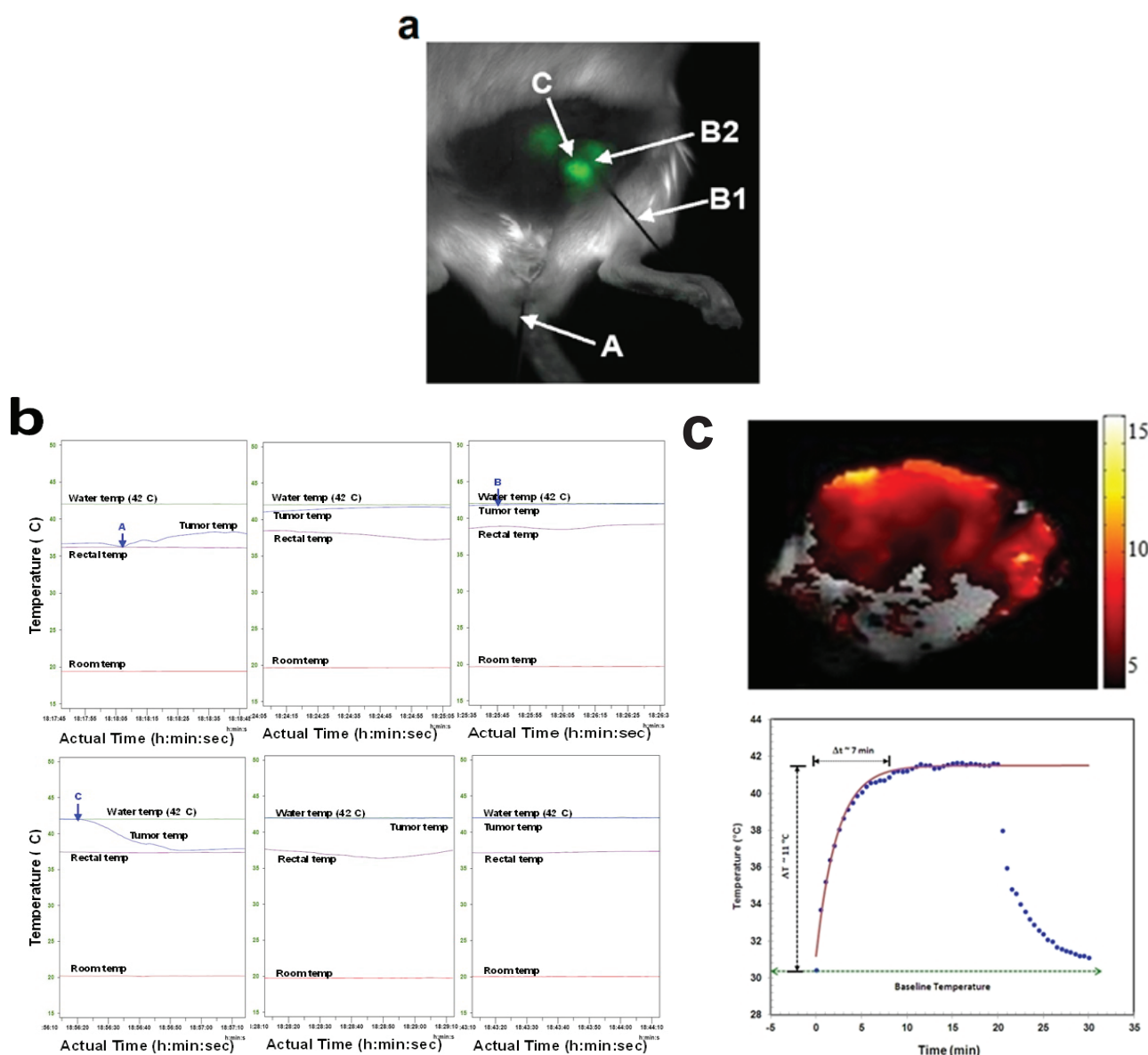


Figure 1: Thermometry setup. **a** 4T1 scrb^{GFP}-shRNA^{GFP} cells (10^4) were injected into the breast pad of a female BALB/c mouse, 7 days later, the mouse was anesthetized and rectal probe (arrow A; Thermocouple sensor, type T-RET-4, Physitemp, Clifton, NJ) was inserted into the rectum to monitor core temperature. A second hypodermic needle microprobe (arrow B1 and B2; MT-29/2, Physi temp) was inserted into the tumor (arrow C) to monitor tumor temperature. A third probe was placed into the water bath. All probes were connected to a 7-channel type T thermocouple inputs connected to a laptop, equipped with temperature acquisition and analysis software (Physitemp). The mouse was then exposed to HT (41°C for 60 min). Arrow C points to the 4T1 breast adenocarcinoma tumor tagged with GFP and visualized using an *in vivo* imaging system (CRI, Cambridge, MA). **b** Temperature kinetics of mice exposed to HT. A tumor bearing female BALB/c mouse was lightly anesthetized and temperature measurements were recorded from 4 temperature probes; probe 1, water temperature (green line); probe 2, tumor temperature (blue line); probe 3, rectal probe (purple line); probe 4, room temperature (red line). All probes are connected to a 7-channel type T thermocouple inputs which is connected to a laptop, equipped with temperature acquisition and analysis software (Physitemp). The mouse was placed into a circulating water bath set at 41.4°C (arrow A; top left panel) and temperature kinetics followed until the tumor temperature reaches 41.0°C (arrow B; top right panel) and terminated 30 minutes later (arrow C; bottom right panel). **c** Nanoshell-mediated hyperthermia. Panel on the left shows the set-up with an 808 nm near-infrared diode laser (Diomed-plus 15, Diomed corp, UK) used to illuminate the tumor surface (10 mm diameter spot size) via a fiber optic cable with a collimating lens 24 hours following intravenous injection of 8×10^8 nanoshells/g body weight. PEG diacrylate (Mx 600, Sartomer, West Chester, PA) was applied over the surface of the tumor as an index-matching agent. Beginning with a tumor core temperature of $\sim 30^\circ\text{C} \pm 1^\circ\text{C}$, ΔT s of $\sim 10\text{C} \pm 1.5^\circ\text{C}$ and $\sim 8^\circ\text{C} \pm 0.5^\circ\text{C}$ in the tumor core and base, respectively were achieved 5-7 minutes following illumination with a laser power of 0.6 W/cm^2 at a 75% duty cycle. Panel on the right shows a representative image of the tumor cross-sectional T2-weighted magnetic resonance image with an overlay of temperature as determined by proton resonance frequency shift calculations and a temperature-versus-time plot obtained using a thermocouple inserted into a tumor in another mouse.

gentle rocking and total Hsp70 content measured by standard sandwich ELISA. Briefly, 96-well microtitre plates (Nunc Immunoplate Maxisorp; Life Technologies) were coated with murine monoclonal anti-human Hsp70 (clone C92F3A-5; StressGen) in carbonate buffer, pH 9.5 ($2\ \mu\text{g/mL}$) overnight at 4°C . Plates were then washed with PBS containing 1%

Tween 20 (PBS-T) and blocked by incubation with 1% bovine serum albumin in PBS-T. Asea-0821 buffer treated supernatant was added and bound Hsp72 was detected by the addition of rabbit polyclonal anti-Hsp70 antibody (SPA-812; StressGen). Bound polyclonal antibody was detected with alkaline phosphatase-conjugated murine monoclonal an-

tibody to rabbit immunoglobulins (Sigma Chemical Co), followed by p-nitrophenyl phosphate substrate (Sigma Chemical Co). The resultant absorbance was measured at 405 nm with a BioRad Benchmark Plus plate reader. Standard dose-response curves were generated in parallel with Hsp70 (0 to 20 000 ng/mL; StressGen), and the concentrations of Hsp70 were determined by reference to these standard curves with ASSAYZ-AP data analysis software (BIOSOFT). The interassay variability of the Hsp70 immunoassays was <10%.

Results

Here we present an example of thermometry data acquired when a single mouse was exposed to HT (Figure 1B). Since all the data could not be placed on one page, we elected to present only representative sections. On initial measurement, tumor and rectal temperatures are approximately similar. At 18:18:05 (arrow A) the animal is placed into the circulating water bath set at 41.4°C (Figure 1B, top left panel). From experience, we have found that this temperature ensures that the tumor temperature is maintained at 41.0°C ± 0.2°C. Once placed into the water bath, the tumor temperature can be seen to rapidly rise (Figure 1B, top middle panel), but it does not reach 41.0°C ± 0.2°C until 7 minutes and 40 seconds later at 18:25:45, arrow B (Figure 1B, top right panel). Therefore, in this representative experiment, with this particular mouse, bearing this particular tumor, the heat-up kinetics was 7 minutes and 40 seconds. We have independently repeated this experiment numerous times and found that the heat-up kinetics ranges from 5-10 minutes. The experiment was stopped after the tumor temperature was maintained at 41.0°C ± 0.2°C for 60 minutes (arrow C; 18:56:20) (Figure 1B, bottom right panel).

In similar experiments with mice injected intravenously with 8 × 10⁸ nanoshells/g body weight of polyethylene glycol coated plasmonic silica-gold core-shell nanoparticles measuring 150 nm in diameter, maximal tumor accumulation via the enhanced permeability and retention effect has been previously demonstrated at 24 hours post-injection. In our experience, focal illumination with a near-infrared laser (Figure 1C) results in tumor-specific elevations of temperature to 41°C in the core of a ~8 mm tumor within 5-7 minutes and can be maintained for over 20 minutes without significant elevations of rectal temperature. This presents an alternative strategy for generation of hyperthermia by capitalizing on the surface plasmon resonance of gold atoms encasing a dielectric silica core tuned to the frequency of an exciting laser in the near-infrared wavelengths where there is minimum absorbance by normal biomolecules such as hemoglobin, melanin and water. The relative non-invasive nature of achieving hyperthermia using laser illumination and monitoring it using magnetic resonance thermometry make this an appealing strategy for clinical applications in superficial tumors [9].

A natural consequence of generating hyperthermia via systemically injected nanoparticles is the lack of spatial and temporal uniformity of temperature attained within tumors (as seen in Figure 1C) due to heterogeneity of nanoparticle distribution, and heterogeneity of laser power density. However, this disadvantage seems to be counterbalanced, to some extent, by some favorable characteristics. We have demonstrated that this form of hyperthermia results in an immediate increase in perfusion (and therefore, oxygenation) of the hypoxic core of tumors, making them more sensitive to radiation. Nanoparticle mediated hyperthermia also causes vascular disruption subsequently and contributes to additional anti-tumor effects. We hypothesized that this is due to the perivascular sequestration of nanoparticles and the sharp gradient of decreasing heat transmitted to tissues further away from the blood vessel. Therefore, nanoparticle-

mediated hyperthermia results in dual modes of radio sensitization via an initial increase in oxygenation of tumors and a subsequent pronounced vascular endothelial (in addition to tumor parenchymal) damage that leads to necrosis [9]. In contrast to other forms of hyperthermia where external energy sources transduce heat within a tumor ("outside-in"), nanoparticle-mediated hyperthermia mediates the elevation of temperature from within the tumor ("inside-out") with heat emanating from perivascularly sequestered nanoparticles thereby creating temperature 'hot-spots' along vasculature rather than heat sinks or 'cold-spots' where blood courses through vasculature at body temperature. This might, in fact, be an advantage when targeting cancer stem cells since the perivascular zone is recognized to be a nidus or a niche for these tumor-initiating cells. Infact, this is precisely what we discovered when we evaluated the possibility that nanoparticle-mediated hyperthermia might preferentially sensitize tumor stem cells to radiation therapy.

We have engineered two constructs and introduced them into baculovirus expression vectors to make functional Hsp72 proteins fused to green fluorescent protein (GFP) in 4T1 murine breast adenocarcinoma cells. We first constructed a short hair-pin RNA (shRNA) sequence which is tagged with GFP and specifically targets intracellular Hsp72, referred to as Hsp72-shRNA^{GFP}. Stable transfection of 4T1 cells with Hsp72-shRNA^{GFP} produces cells we refer to as 4T1 (Hsp72-shRNA^{GFP}) cells. The second construct was a control sequence, also referred to as a scrambled sequence which was also tagged with GFP. This sequence is constructed so as not to target any known sequence in the mouse genome and is referred to as scrb-shRNA^{GFP}. Similar stable transfection of 4T1 cells with scrb-shRNA^{GFP}, produces control cells, we refer to as 4T1 (scrb-shRNA^{GFP}) cells. Both cell lines grow in a normal fashion in cell culture, as compared to wild type 4T1 cells, which are cells not transfected with any shRNA, and referred to by us as 4T1^{wt} cells. To determine the functional activity of the two constructs, 4T1 (scrb-shRNA^{GFP}) cells, 4T1(Hsp72-shRNA^{GFP}) cells and 4T1^{wt} cells were exposed to HT (41°C, 60 min) or maintained at 37°C for a similar time. To obtain maximal Hsp72 expression, cells were incubated for an additional 24 h in a 37°C incubator. We demonstrated that the Hsp72-shRNA^{GFP} construct effectively silences the baseline expression of Hsp72 (Figure 2, lane 5) and the heat inducible expression of Hsp72 (Figure 2, lane 6). As compared to 4T1 (scrb-shRNA^{GFP}) control cells or 4T1^{wt} cells, in which baseline levels of Hsp72 can be observed (Figure 2, lanes 3 and 1, respectively) and HT treatment induced the expression of Hsp72 (Figure 2, lane 4 and 2, respectively).

To test whether Hsp72 traffics *via* the endocytic pathway, we exposed 4T1 (scrb-shRNA^{GFP}) cells to HT and followed Hsp72 trafficking using confocal microscopy, immunoprecipitation and Western blot analysis of subcellular fractions containing various endolysosomal fractions. Since HT treatment stimulates a significant increase in Hsp72 expression in cells as early as 1h after HT treatment [10], we began analyzing Hsp72 trafficking 10 min after HT (41°C, 60 min) treatment was completed. We demonstrated that as early as 10 min after exposure of 4T1 (scrb-shRNA^{GFP}) cells to HT (41°C 60 min), Hsp72 colocalized with Rab4 proteins (Figure 3A). Rab4 is a small GTPase protein known to be associated with early endosomes (EE) and to regulate membrane recycling in fibroblasts [11,12]. Rab4 was expressed in the nucleus 10 min after exposure of cells to HT (Figure 3A, middle panel), and Hsp72 was observed both in the nucleus and cytoplasm (Figure 3A, top panel). When the micropictogram images were merged, Hsp72 was observed to colocalize with Rab4 proteins in the cytoplasm (Figure 3A, bottom panel).

To confirm that Hsp72 colocalizes with Rab4 within EE, 10 minutes after exposure to HT was completed cells were lysed and

immunoprecipitated with anti-Hsp72 and the recovered antibody coated beads were further probed with antibodies against Rab4, Rab5, Hsp72, LAMP1 or Rab11 by Western blot analysis (Figure 3B). We obtained positive bands when membranes were probed with anti-Rab4 and anti-Rab-5 Mab (localized on EE and on the cytoplasmic face of the plasma membrane, are involved in the process of EE fusion), but not with anti-LAMP1 Mab (a protein associated with LE) or anti-Rab-11 Mab (associated with trans-Golgi to plasma membrane transport) (Figure 3B). Since our results suggest that an early event in HT-induced Hsp72 trafficking (i.e., 10 min) is entry of Hsp72 into EE and not LE. We hypothesized that pre-treatment of cells with glibenclamide, a specific inhibitor of endosome-to-plasma membrane transport, before HT treatment would not affect this early event, since endosome-to-plasma membrane transport is a late event prior to Hsp72 release from cells into the microenvironment. As expected, Hsp72 did not immunoprecipitate within subcellular fractions enriched for EE when cells were pre-treated with glibenclamide (Figure 3C). Most proteins

are transported to the extracellular milieu *via* the classical protein transport pathways dependent on the ER-Golgi transit [13]. However, we demonstrated that monensin (compound known to block transport out of the Golgi apparatus), brefeldin A (inhibitor of anterograde transport from ER to Golgi), thapsigargin (an ATPase inhibitor that specifically depletes calcium from the ER) and tunicamycin (an inhibitor of *N*-glycosylation) were each unable to suppress HT treatment-induced Hsp72 release (Table 1). Depletion of intracellular Ca²⁺ using BAPTA-AM (an intracellular Ca²⁺ chelator) but not extracellular Ca²⁺ (using EGTA, an extracellular Ca²⁺ chelator) resulted in inhibition of HT treatment-mediated Hsp72 release (Table 1). Taken together, these results support the conclusion that HT treatment-induced release of Hsp72 is mediated *via* a non-classical protein transport pathway that is dependent on intracellular Ca²⁺ (Table 1).

The plasma membrane of cells is partially composed of arranged domains, known as lipid rafts [14]. Evidence that the active release of Hsp72 requires intact lipid raft formation was provided in experiments

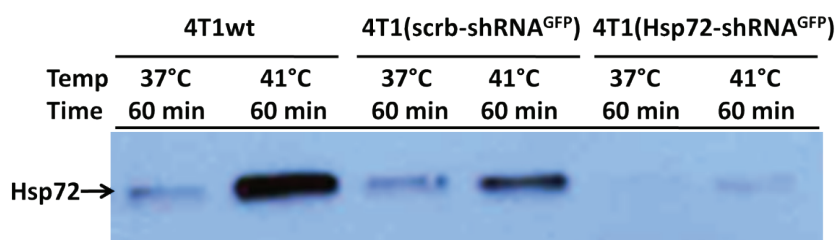


Figure 2: Hsp72-shRNA^{GFP} construct effectively silences baseline and heat-induced intracellular Hsp72 expression in stably transfected 4T1 cells. 4T1 cells were stably transfected with Hsp72-shRNA^{GFP} (lanes 5-6) or scrb-shRNA^{GFP} (lanes 3-4) or not transfected 4T1wt (lanes 1-2). Cells were exposed to HT treatment (41°C, 60 min) or maintained at 37°C for 60 min, then incubated for an additional 24 h in a 37°C incubator. Cells were lysed and proteins separated in a 10% SDS-PAGE then transferred onto a PVDF membrane and immunoblotted with anti-Hsp72.

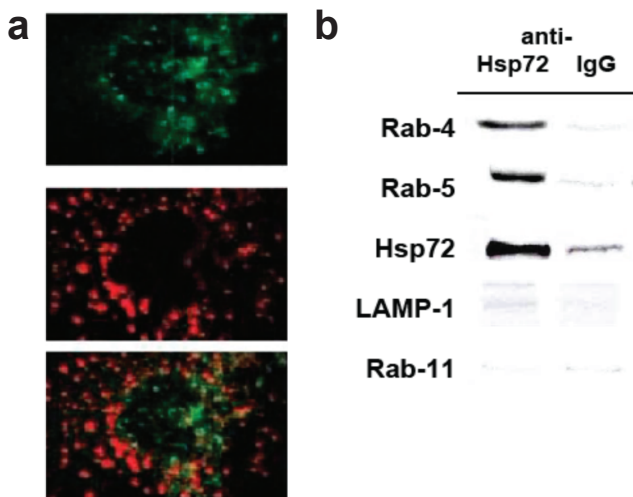


Figure 3: Four hours post hyperthermia (HT) treatment Hsp72 colocalizes within early endosomes (EE). **a** Anti-Rab4-TRITC was loaded into live 4T1 (scrb-shRNA^{GFP}) cells using the Chariot delivery system. Cells were then exposed to HT treatment (41°C, 60 min). Ten minutes later, cells were fixed and permeabilized and fluorescence measured using confocal microscopy. **b** Hsp72 immunoprecipitates with Rab4 and Rab5 but not Rab11 or LAMP1 10 after HT treatment. 4T1 (scrb-shRNA^{GFP}) cells (10⁶) were exposed to HT (41°C, 60 min) and incubated at 37°C for a further 10 min. Cells were lysed and immunoprecipitated with anti-Hsp72 conjugated Sepharose beads and proteins separated in a 10% SDS-PAGE then transferred onto a PVDF membrane and immunoblotted with primary antibodies against Rab4, Rab5, Hsp72, LAMP1 and Rab11. **c** Glibenclamide inhibits trafficking of Hsp72 into early endosomes. 4T1 (scrb-shRNA^{GFP}) cells were pre-treated 10 nM glibenclamide for 30 min at 37°C. Cells were then exposed to HT (41°C, 60 min), lysed and subcellular fractions containing early and LE were recovered by serial centrifugation over a sucrose gradient. Subcellular fractions containing early endosomes (EE) and late endosomes (LE) were recovered over sucrose gradient at the 35/25% and 25% interfaces, respectively. Proteins were separated in a 10% SDS-PAGE and immunoblotted with anti-EEA-1 or anti-Hsp72. **d** HT-induced Hsp72 release requires an intact lipid rafts. 4T1 (scrb-shRNA^{GFP}) cells (10⁶) were pre-treated with M&D (2.5 mM, lanes 1 and 2) for 6 h at 37°C prior to exposure for 60 min to 41°C (HT; lanes 2 and 4) or maintained at 37°C (control; lanes 1 and 3) and then transferred to a 37°C for a further 24 h. Supernatant was then recovered (bottom panel) or cells lysed (top panel) and Hsp72 expression measured by Western blot analysis using anti-Hsp72 Mab. The intensity of the bands were analyzed by densitometry with a video densitometer (Chemilmager™ 5500; Alpha Innotech) using the AAB software (American Applied Biology).

in which pre-exposure of cells to methyl β -cyclodextrin (M β D), a compound known to disturb lipid raft organization by specifically depleting cholesterol, significantly inhibited HT treatment-induced Hsp72 release into the supernatant (Figure 3D, bottom panel, lanes 1 and 2), as compared to cells pre-treated with PBS alone (Figure 3D, bottom panel, lanes 3 and 4). Disruption of lipid rafts using M β D effectively resulted in significant accumulation of Hsp72 within the cells both under control conditions and in response to exposure to HT (Figure 3D, top panel, lanes 1 and 2), as compared to cells pre-treated with PBS (Figure 3D, top panel, lanes 3 and 4). Taken together, we interpret the data presented as demonstrating that; 1) HT treatment induces Hsp72 trafficking within endosomes, 2) one of the earliest events in HT treatment-induced Hsp72 trafficking is entry of Hsp72 into EE and not LE compartments, 3) there is a requirement for intracellular Ca²⁺, and 4) lipid rafts are important for efficient release of Hsp72 from cells.

The content of the Hsp72-containing exosomes is critically dependent upon the type of stressor (HT or RT treatment) to which tumor cells are exposed to induce Hsp72 release. We demonstrated that exposure of 4T1 (scrb-shRNA^{GFP}) cells to HT treatment result in the release of exosomes containing significantly higher levels of Hsp72, as compared to cells maintained under control conditions of 37°C (Figure 4B). When the concentration of free Hsp72 in the supernatant was measured using the classical sandwich ELISA, similar results were obtained showing that HT >> RT > control for the release of Hsp72 (data not shown). Western blot analysis of the 1.17 g/ml density

exosome fraction (obtained from sucrose gradient ultracentrifugation) revealed that HT treatment induces a relatively higher expression of Hsp72 within the exosomes than either cells exposed to RT (I didn't see any RT data here) or cells maintained in control condition (Figure 4A). Characterization of the internal content of the Hsp72 containing exosomes revealed the presence of Hsp73 (the constitutively expressed HSP70 family member, known to be expressed in exosomes), tubulin (a cytoplasmic protein expressed within exosomes), milk fat globule-EGF-factor 8 (MFG-E8; a protein known to mediate the engulfment of apoptotic cells by activated macrophages), but not calnexin (an ER-resident, known not to be expressed in exosomes). We interpret these data to suggest that the Hsp72 containing exosomes originate

Pretreatment ¹	Hsp72 concentration (ng/ml) ² after	
	Control (37°C, 60min)	HT (41°C, 60 min)
Control	10.9 ± 4	363.4 ± 12*
Monensin	12.5 ± 3	353.9 ± 13*
Brefeldin A	13.1 ± 2	381.4 ± 14*
Tunicamycin	11.7 ± 3	370.9 ± 17*
Thapsigargin	19.3 ± 2	366.8 ± 12*
BAPTA-AM	14.1 ± 3	34.5 ± 16
EGTA	13.8 ± 2	365.6 ± 11*

¹4T1 (scrb-shRNA^{GFP}) cells were pre-treated with 10 μ M Monensin, 10 μ M Brefeldin A, 20 μ M Tunicamycin, 1 μ M Thapsigargin, 20 μ M BAPTA-AM, 1.5 mM EGTA for 6 h at 37°C.

²Cells were exposed to HT treatment (41°C, 60 min) or maintained at 37°C (Control) for an additional 24 h at 37°C. Supernatant from the cell culture was recovered, centrifuged to clear floating cells and cellular debris and treated 1% Lubrol for 10 min at 4°C with gentle rocking, after which Hsp72 content was measured by a modified Hsp72 ELISA. Data represent the mean Hsp72 concentration (ng/ml \pm SD) and is the sum of two independent experiments performed in quadruplicates.

Table 1: Intracellular Ca²⁺ is required for HT treatment-induced Hsp72 release.

Treatment ¹	Hyperthermia exposure (temperature, time)	Tumor volume (mm ³ \pm SD)
PSB	25°C, 60 min	492 \pm 48
Ab46	25°C, 60 min	489 \pm 45
Iso-ctrl	25°C, 60 min	455 \pm 50
PSB	41°C, 60 min	337 \pm 33
Ab46	41°C, 60 min	488 \pm 39*
Iso-ctrl	41°C, 60 min	345 \pm 24

¹Female BALB/c mice were injected with 10⁴ 4T1(Hsp72-scrb^{GFP}) cells into the breast pad. When tumors grew to ca. 100mm³, mice were injected i.p. with either, PBS, anti-Hsp72 (Ab46) or isotype control (Iso-ctrl) for 3 consecutive days.

²After treatment, mice were exposed to HT treatment (41°C water bath for 60 min) or maintained at ambient temperature control water (25°C water bath for 60 min).

³Tumor volume was monitored using an electronic caliper 28 days after injection of tumors.

*, p<0.05; vs respective PBS and isotype control (13 mice/group).

Table 2: Depletion of Hsp72 abrogates HT treatment-induced tumor regression.

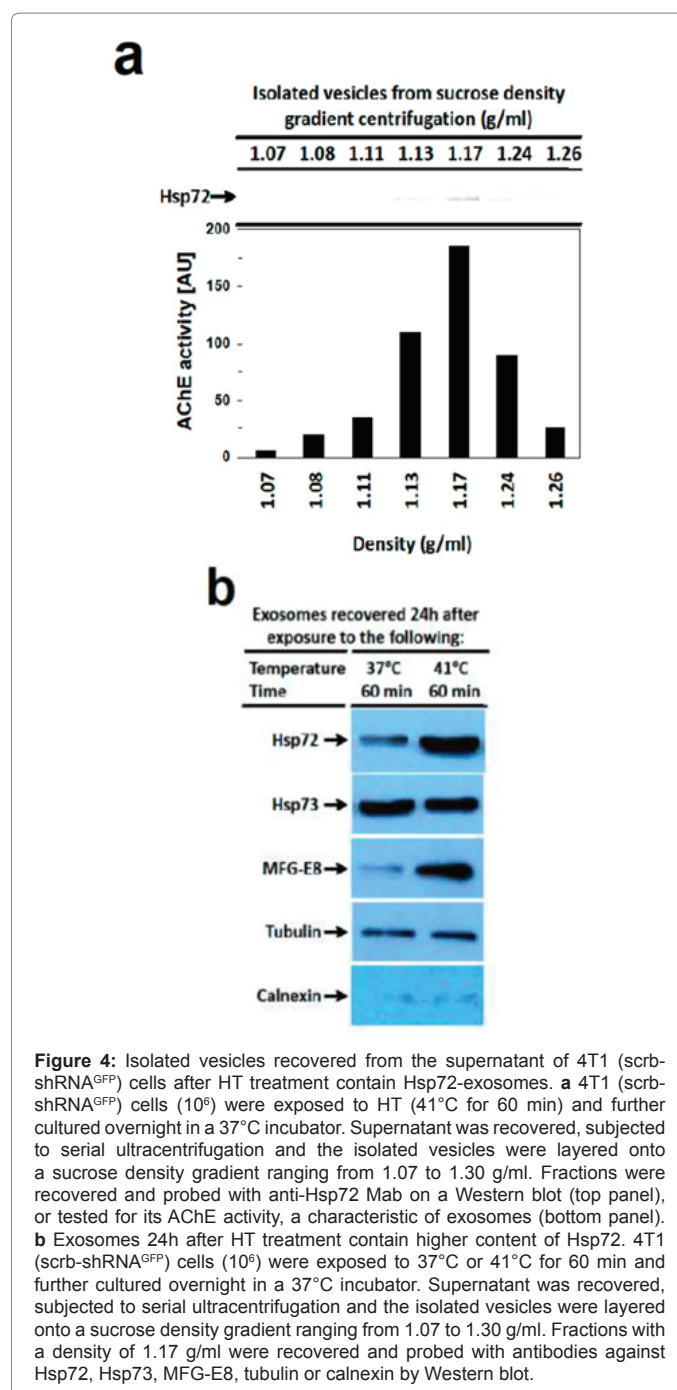


Figure 4: Isolated vesicles recovered from the supernatant of 4T1 (scrb-shRNA^{GFP}) cells after HT treatment contain Hsp72-exosomes. **a** 4T1 (scrb-shRNA^{GFP}) cells (10⁶) were exposed to HT (41°C for 60 min) and further cultured overnight in a 37°C incubator. Supernatant was recovered, subjected to serial ultracentrifugation and the isolated vesicles were layered onto a sucrose density gradient ranging from 1.07 to 1.30 g/ml. Fractions were recovered and probed with anti-Hsp72 Mab on a Western blot (top panel), or tested for its AChE activity, a characteristic of exosomes (bottom panel). **b** Exosomes 24h after HT treatment contain higher content of Hsp72. 4T1 (scrb-shRNA^{GFP}) cells (10⁶) were exposed to 37°C or 41°C for 60 min and further cultured overnight in a 37°C incubator. Supernatant was recovered, subjected to serial ultracentrifugation and the isolated vesicles were layered onto a sucrose density gradient ranging from 1.07 to 1.30 g/ml. Fractions with a density of 1.17 g/ml were recovered and probed with antibodies against Hsp72, Hsp73, MFG-E8, tubulin or calnexin by Western blot.

from cytosol, suggestive of the endolysosomal trafficking pathway, as opposed to ER-Golgi trafficking pathway.

For *in vivo* studies, we have used the 4T1 breast adenocarcinoma mouse model, because tumor growth and metastatic spread of 4T1 cells very closely mimic human breast cancer. When injected into the abdominal breast gland of female BALB/c mice, 4T1 cells spontaneously produces highly metastatic tumors that can metastasize to the lungs, liver, lymph nodes and brain while the primary tumor is growing *in situ*. The primary tumor does not have to be removed to induce metastatic growth making this a very good breast cancer tumor model to study mechanisms of HT treatment stimulated tumor regression.

We next tested the ability of the two 4T1 cell types to grow in mice and whether we can effectively image the fluorescent signal non-invasively in mice using an *in vivo* imaging system for small animals. Using the Meastro™ *in vivo* imaging system (CRI, Cambridge, MA), we successfully imaged the growth of 4T1 scrb-shRNA^{GFP} cells injected into the breast pad of female BALB/c mice. As early as 2 days after injection of 10⁴ cells into the breast pad of female BALB/c mice, significant GFP signal was detected indicating the presence of 4T1 cells. We show that the GFP signal is still significant up to 28 days post tumor injection (data not shown). To visualize the effect of HT treatment on tumor growth *in vivo*, on day 7 post tumor injection, animals were exposed to a single dose of HT treatment (41°C, 60 min) or maintained at ambient temperature and tumor growth monitored using the *in vivo* imaging system. Whole body HT exposure was avoided by placing the mouse in a Styrofoam box, with a space cut out in which the tumor is directly exposed to heated water. Overheating was avoided by closely monitoring the rectal thermistor probes and at any sign that the core temperatures were rising to critical temperatures (2°C above normal body temperature, 36°C), a fan and ice were at hand to cool the animals in the box. We have extensive previous experience with this procedure [15,16]. After mice are placed in a 41°C water bath, it normally takes between 7-10 min for the thermistor inserted into the tumor to register 41°C, at which time we start timing for the 60 min to obtain HT exposure. To visualize HT treatment-induced release of Hsp72 *in vivo*, we used a higher magnification of the imaged tumors. We demonstrate that, as early as 30 min after exposure of the tumors to HT treatment, there is the appearance of GFP-tagged Hsp72 in the breast tissue, as determined by a green haze around the tumor (Figure 5A, open arrows).

To confirm that the green fluorescence imaged is GFP-tagged Hsp72, we recovered serum at various times post exposure and measured the amount of Hsp72 in the plasma using conventional “sandwich” ELISA. We demonstrated that 1 hour post exposure of mice to HT treatment there was a significant increase in Hsp72 scrb-shRNA^{GFP} in plasma samples recovered from mice exposed to HT, as compared to unheated mice (145.8 ng/ml ± 9.0 ng/ml versus 1.9 ng/ml ± 0.5 ng/ml, respectively) as judged by Hsp72 ELISA (Figure 5B). Since, GFP is known to minimally stimulate the immune system, the entire experiment was repeated in age and sex matched BALB/c mice, which have a defect in the immune system (data not shown). To determine whether addition of GFP to Hsp72 adversely affects its ability to be released from tumor cells in response to HT treatment, we measured plasma Hsp72 levels in the blood of tumor bearing mice. We demonstrate that Hsp72 release from 4T1 scrb-shRNA^{GFP} (GFP-tagged) cells in response to exposure to HT is consistently less than from 4T1 wild type controls (non-tagged cells). However, statistical analyses using a 2-tailed Student's *t*-test demonstrate that this reduction is not statistically significant (Figure

5B). Therefore, these results would support the conclusion that this reduced efficiency in Hsp72 release will not significantly induce a confounding factor to interpretation of our studies, nor will it negate the significance of future findings on the role of HT treatment-induced Hsp72 trafficking within tumors and its release *in vitro* or its relative contribution to tumor killing *in vivo*. To demonstrate that tumor-derived Hsp72 plays an important role in HT treatment-induced tumor regression, we performed an experiment in which circulating Hsp72 was eliminated by injecting mice with Hsp72 blocking antibody (Ab46) for 3 consecutive days before exposure to HT, and then once a week for the remainder to the experiment. Serum collected at various times confirmed the effectiveness of the blocking antibody (Table 2). We also demonstrated that the elimination of Hsp72 abrogated the tumor regression effects of HT treatment and resulted in the significant increase in tumor growth ($p < 0.05$) as compared to mice injected with PBS or isotype controls (Table 2). We concluded that these results suggest that Hsp72 plays an important role in HT treatment-induced tumor regression.

Discussion

The ability of hyperthermia (HT) treatment to enhance the therapeutic efficacy of radiotherapy (RT) was demonstrated over two decades ago. In both a preclinical animal tumor model and in clinical settings, combined HT and RT treatment resulted in synergistic reduction in tumor growth and enhanced survival relative to RT alone [17]. Results from Phase III clinical trials randomizing between RT treatment and RT plus HT treatment as primary treatment in patients with locally advanced cervical carcinoma provide evidence for significantly improved complete response rates and overall survival for the combination treatment [18-20]. The finding that HT treatment enhances the activity of cisplatin *in vitro* [21,22] led to clinical trials which demonstrated increased response rates and survival in patients with relapsed ovarian carcinoma [23] and recurrent cervical carcinoma without added toxicity [24,25]. Results from subsequent Phase I and II trials of cisplatin, RT and HT treatment supported the value of the triple-modality approach [26-28]. Recently, Phase II studies on the efficacy and toxicity of adding locoregional HT to cisplatin and RT in patients with advanced cervical carcinoma in the U.S., Norway and The Netherlands were reported, demonstrating complete remission in 90% of patients, and after a median follow-up of 538 days, 74% of patients remained alive without signs of recurrence with an overall survival rate of 84% [29]. The findings that HT treatment stimulates the release of tumor-derived heat shock proteins (HSP) [30-33] and augments potent immune responses [3-5,8,34-41], in part, has been proposed as the primary reason for the effectiveness of HT treatment. However, the exact mechanism is incompletely understood.

HT-induced intracellular Hsp72 trafficking occurs *via* the endocytic pathway and Hsp72 is released in two forms; first within highly immunogenic exosomes, but also as free Hsp72 chaperoning tumor-associated antigens (TAA). To develop pharmacological strategies that will effectively increase the production and release of tumor-derived Hsp72 in response to HT treatment, the intracellular trafficking of Hsp72 must first be understood. Most secreted proteins are secreted from cells because they encode an N-terminal, hydrophobic “leader” sequence. This ensures that the translated proteins with such leader sequences become inserted into endoplasmic reticulum (ER) membranes and allows their entry into the secretion pathway [42]. The leader sequence is used to allow penetration of the ER membrane and draw in the remainder of the protein. The protein then traffics within the confines of lipid-bounded organelles and vesicles, until these structures

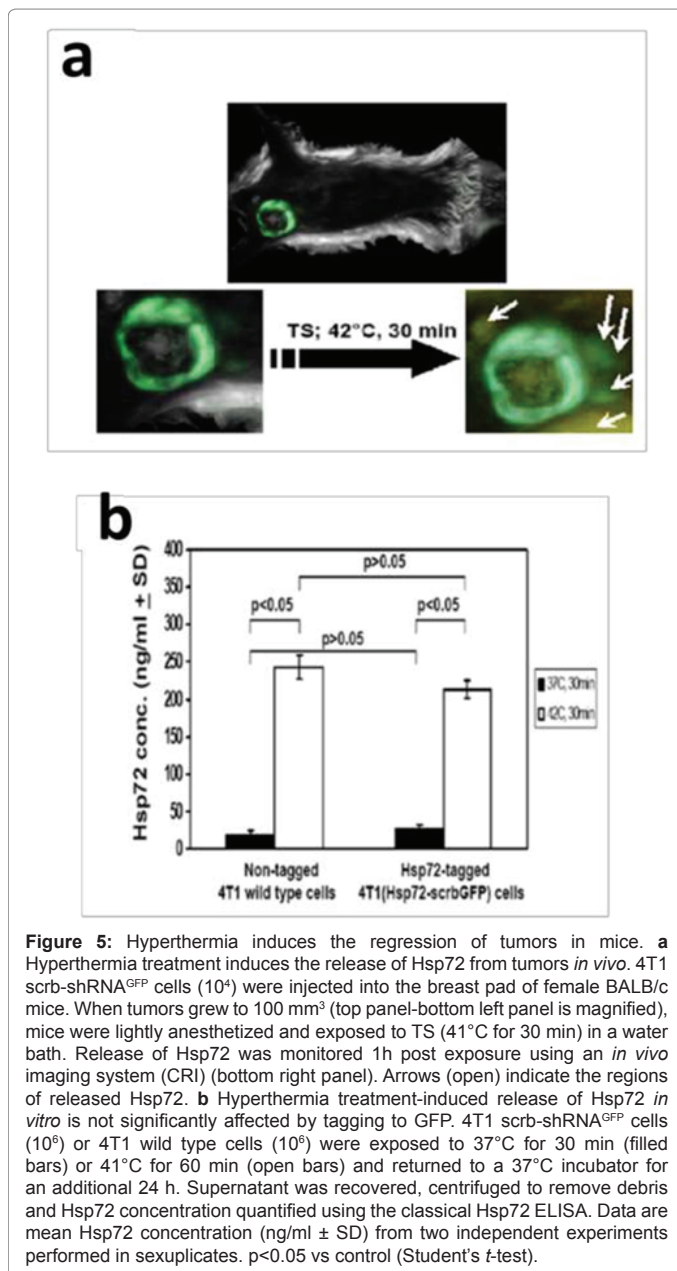


Figure 5: Hyperthermia induces the regression of tumors in mice. **a** Hyperthermia treatment induces the release of Hsp72 from tumors *in vivo*. 4T1 scrb-shRNA^{GFP} cells (10^4) were injected into the breast pad of female BALB/c mice. When tumors grew to 100 mm² (top panel-bottom left panel is magnified), mice were lightly anesthetized and exposed to TS (41°C for 30 min) in a water bath. Release of Hsp72 was monitored 1h post exposure using an *in vivo* imaging system (CRI) (bottom right panel). Arrows (open) indicate the regions of released Hsp72. **b** Hyperthermia treatment-induced release of Hsp72 *in vitro* is not significantly affected by tagging to GFP. 4T1 scrb-shRNA^{GFP} cells (10^5) or 4T1 wild type cells (10^5) were exposed to 37°C for 30 min (filled bars) or 41°C for 60 min (open bars) and returned to a 37°C incubator for an additional 24 h. Supernatant was recovered, centrifuged to remove debris and Hsp72 concentration quantified using the classical Hsp72 ELISA. Data are mean Hsp72 concentration (ng/ml ± SD) from two independent experiments performed in sexuplicates. $p < 0.05$ vs control (Student's *t*-test).

fuse with the plasma membrane and their contents are released into the extracellular spaces [42].

The major problem of understanding Hsp72 trafficking and release from cells is that the genes encoding Hsp72 do not encode ER signal sequence. Therefore, Hsp72 cannot effectively utilize this classical protein secretion pathway to gain access to the extracellular milieu. This is not, however, unique for Hsp72. A non-classical protein trafficking and secretion pathway is also utilized by other proteins, including interleukin-1 β (IL-1 β), IL-1 α , IL-18, IL-33 and IL-1 receptor antagonist IL-1Ra [43]. These proteins do not encode a leader sequence, however, they are still able to accomplish their primary function as secreted proteins to interact with receptors on adjacent or distant target cells [43]. Studies of IL-1 β secretion indicate three potential mechanisms by which this mediator is secreted, including: (a) lysis of IL-1 β containing secretory cells and release of contents, (b) cell surface blebbing and release of IL-1 β in microvesicles that lyse in the extracellular fluid and

(c) entry of IL-1 β into intracellular structures known as endolysosomes that transport the cytokine to the cell surface where they then fuse with the plasma membrane and release the contents upon fusion [44]. We, and other, have demonstrated that each of these mechanisms may be utilized for Hsp72 release [7,8,45-47]. For therapeutic gain, the release of Hsp72 from cells by necrotic cell death rather than apoptotic cells death is suggested to enhance immunogenicity [48,49]. Mild levels of heat shock, within the fever range lead to Hsp72 release while more severe conditions inhibit release, consistent with the inactivation of a protein-based secretion mechanism [7]. Severe heat shock (45°C to 55°C) induces delayed necrosis and a gradual release of Hsp72 as necrosis develops [7].

The elucidation of intracellular trafficking of Hsp72 has been undertaken by several groups, and studies point to an important role for the endolysosomal transport system [7,8,45-47]. Endosomes are defined as membrane-bound compartments inside cells, roughly 300 nm to 400 nm in diameter, which are responsible, in part, for the sorting of endocytosed material before transport to lysosomes or material which is to be secreted from cells [50]. There are various kinds of endosomes, including the early endosomes (EE) which are small irregularly shaped intracellular vesicles to which endocytosed molecules are initially delivered. EE are phenotypically characterized by the presence of Rab5 (a key regulator of endocytosis that orchestrates the recruitment of multiple effector proteins on the EE membrane to regulate organelle tethering, fusion, and microtubule-dependent motility), early endosome autoantigen-1 (an early endosome marker), and transferrin receptors (Zerial and McBride, 2001). Recycling endosomes (RE) are organelles consisting of networks of 60 nm tubules organized around the microtubule organizing centre in some cell types. RE transport receptors from late endosomes (LE) back to the plasma membrane for recycling and are also involved in membrane trafficking. RE are identified by the presence of AP-1B, which is required for the tethering of transport carriers to the basolateral plasma membrane [51,52], Rab8 which regulates the traffic of newly synthesized AP-1B-dependent cargo and SNARE (soluble *N*-ethylmaleimide-sensitive factor attachment protein receptors), which are key regulators of vesicular membrane traffic [53]. LE are characterized as prelysosomal endocytic organelle differentiated from EE by lower luminal pH and different protein composition. LE are more spherical than early endosomes and are mostly juxtannuclear, being concentrated near the microtubule organizing center. LE are identified by the presence of Rab-7 (a protein associated with late endosomes to lysosomes), Rab-9 (a protein associated with late endosomes to trans-Golgi), Rab-11 (a late endosome protein associated with trans-Golgi to plasma membrane transport), lysosome associated membrane protein (LAMP1; a protein associated with late endosomes), and p14 (a protein which functions as an endosomal adaptor for MP1 and is required to attach MP1 to late endosomes) [54,55].

Lysosomes (Ly), in contrast, are organelles that contain digestive enzymes (acid hydrolases). Their basic function is to digest excess or worn-out organelles, food particles, and engulfed viruses or bacteria. Ly are identified by the presence of LAMP2 (lysosomal associated protein 2) which is involved in the direct uptake of cytosolic proteins in lysosomes and participates in the endocytic pathway. The protein is localized mainly to lysosomes; however, under certain conditions, it can also be detected in the plasma membrane. Interestingly, the level of LAMP2 protein expressed on the surface of tumor cells has been found to correlate with the tumor's metastatic potential [56,57]. Multivesicular bodies (MVB) are specialized endosomes that transit from EE and RE to LE and/or Ly. Internalized membrane receptors and their ligands are

sorted into microdomains on the limiting membrane of MVB, which are invaginated as internal vesicles into the lumen of the MVB. Hence, they are called multivesicular bodies. As the MVB mature into lysosomes, they fuse with pre-lysosomes and intraluminal cargos and are degraded by lysosomal acid hydrolases. MVB are also involved in secretion, in which intraluminal vesicles are pinched off the limiting membrane as exosomes [58]. Therefore, the intracellular trafficking pathway utilized by Hsp72 will be shown to be an active mechanism that is independent of *de novo* Hsp72 synthesis or cell death and will involve transit through endolysosomal compartments requiring the participation of the ABC-family transporter proteins and P2X7R followed by binding to surface bound lipid rafts as Hsp72 is released from cells.

The content of Hsp72-exosomes and free Hsp72 chaperoning tumor-associated antigen (Hsp72-TAA) is critically dependent upon the type of stressor used to promote tumor cell-dependent Hsp72 release. In *in vitro* experiments, we demonstrated that hyperthermia induces the release of Hsp72 in two forms, as free Hsp72 still chaperoning peptides from cells (Hsp72-TAA) and as Hsp72 contained within exosomes [8,45].

Once released from cells, Hsp72 has been demonstrated to exert a profound effect on cells of the immune system, known as the chaperokine activity. Chaperokine, is a term recently coined to better describe the unique function of extracellular Hsp72 as both chaperone and as a cytokine [3,6,59,60]. The consequence of binding and signaling is the stimulation of a potent and long lasting immune response. Extracellular Hsp72 induces a spectrum of immune responses and the list continues to grow. Several immune effector functions are attributed to various sources of Hsp72, including recombinant bacterial, viral and parasitic sources, Hsp72 from human, mouse and non-human primate tissue and their targets. As early as 2-4 hours post exposure of antigen presenting cells (APC) to extracellular Hsp72 (eHsp72), there is significant release of cytokines, including TNF- α , IL-1 β , IL-6 and IL-12 [61,62] and GM-CSF [34]; nitric oxide, a potent apoptogenic mediator [35]; chemokines, including MIP-1, MCP-1 and RANTES [35,36]. This part of the immune response does not require Hsp72 to be associated with peptide, since both peptide-bearing and non-peptide-bearing eHsp72 is capable of inducing pro-inflammatory cytokine production by APCs [37]. However, peptide is required for development of the subsequent specific CD8⁺ CTL responses [30-32]. eHsp72 induces DC maturation by augmenting the surface expression of CD40, CD83, CD86 and MHC class II molecules on DC [33,61,63,64] and migration of DC [65] and NK cells [45] towards the eHsp72.

Srivastava's group demonstrated that vaccination of mice with Hsp72 derived from Meth A sarcoma, but not from normal tissues, renders mice immune to challenge with Meth A sarcoma [66]. It is reported that the immunogenicity was dose dependent and tumor specific and that treatment of the antigenically active Hsp72 preparation with ATP followed by removal of low-molecular weight material leaves Hsp72 intact, but results in loss of antigenicity [66]. These studies formed the basis for Phase III clinical trials for the treatment of patients with stage IV melanoma [67], stage IV metastatic renal cell carcinoma (RCC) patients undergoing nephrectomy [68], and Phase I clinical trials using autologous tumor-derived HSP from resected pancreas adenocarcinomas [69]. The results from this study demonstrated that it is, indeed, feasible to use autologous tumor-derived HSP in patients with pancreatic adenocarcinomas and showed a significant increase in immune parameters. The authors reported that 3 out of 10 treated patients were alive and disease-free at 2.6, 2.7, and 5.0 years' follow-up [69]. Hsp72 released in response to exposure to HT contains

significantly greater concentration of bioactive mediators (cytokines, chemokines and costimulatory molecules), HSP and TAA than Hsp72 released in response to radiotherapy. A compound STA-4783 (Synta Pharmaceuticals, Boston, MA) in a double-blind, randomized, controlled Phase IIB melanoma study conducted in 21 centers in the U.S. in combination with paclitaxel, demonstrated significantly increased serum Hsp72 levels, decreased extent of metastasis and a doubling of progression-free survival (Third International Melanoma Research Congress, 2006).

In general, HT treatment has been shown to induce tumor cell death at temperatures between 40°C to 44°C [70]. The reason HT treatment does not cause significant cell death at similar temperatures in normal cells seems to lie in the difference in physiology between the two cells. One important difference is the architecture of the vasculature of solid tumors which is chaotic, resulting in regions with hypoxia and low pH, not normally found in normal tissue [71]. It has been suggested that, at temperatures more than 40°C, HT treatment functions by inhibiting the repair of double strand break (DSB) [72,73]. Recent studies from the Dynlacht lab demonstrated that exposure of human U-1 melanoma cells to HT treatment (42.5°C) results in the rapid translocation of Mre11, Rad50, and Nbs1 from the nucleus to the cytoplasm [74]. This is potentially important because Mre11 and Rad50 have been shown to play an important role in DSB repair, and Nbs1 seems to be involved in signaling the damage [75].

Several mechanisms appear to be responsible for the supra-additive effect of the combination of radiotherapy (RT) and hyperthermia (HT) treatments in promoting tumor regression *in vivo*. The additive complementary effect comes from the sensitivity of cells in the hypoxic, low pH areas, and the cells in S-phase, which are both relatively radio resistant. Hyperthermia may cause an increased blood flow, which may result in an improvement in tissue oxygenation which then results in a temporally increased radio sensitivity. Experimental studies have also shown, for almost all cell lines studied, that hyperthermia also potentiates radiation effects. The most important mechanism for this interactive effect is that the consequence of hyperthermia led to an interference with the cellular repair of radiation-induced DNA damage, probably by an adverse effect on cellular proteins. The thermal enhancement ratio for radiation-induced cell kill is greater under hypoxic conditions, increases with higher temperatures and longer exposure times, and decreases with longer time-intervals between exposures to the two modalities. Maximum thermal enhancement ratios are obtained when radiation and hyperthermia are applied simultaneously, but this has been found for both tumor and normal tissues. *In vivo* studies have demonstrated that the effect of radiotherapy can be enhanced by HT treatment by a factor of between 1.2 and 5. When tumor and normal tissue are heated to the same degree, maximum therapeutic gain will be obtained with a time interval between the two treatments. Overall, hyperthermia is probably the most potent radio sensitizer known to date.

Conclusions

Our results suggested that hyperthermia stimulated tumor regression, in part, by stimulating the release of Hsp72 from tumors which is taken up by APC preparatory to activating CD8⁺ CTL cytotoxic responses against tumors. These mechanistic studies provide the framework for development of pharmacological strategies that can be used to increase the production and release of tumor-derived HSP in combination with HT treatment. Once such strategies become available, there is a promise that the effectiveness of the current triple-modality approach to treating cancer will be augmented, thereby further increasing complete response rates and overall survival. This will provide the scientific

rationale for using Hsp72-releasing compounds in the triple-modality approach. Since HSP are found in all cellular organisms, it is also expected that what is learned will likely be applicable to the prevention/treatment of diseases of agriculturally relevant animals. It is expected to contribute to the broader understanding of intracellular trafficking pathways as an approach to therapy. Furthermore, a better fundamental understanding of how HT treatment induces Hsp72-mediated anti-tumor responses can be anticipated.

Acknowledgement

This work was funded in part by institutional support from Morehouse School of Medicine and U54 CA118638 (to P.K.) and institutional support from Scott and White Memorial Hospital and Clinic, Texas A&M Health Science Center College of Medicine, the Central Texas Veterans Health Administration, the US National Institutes of Health grant RO1CA91889, an Endowment from the Cain Foundation and University of Dammam (to A.A.). The authors alone are responsible for the content and writing of the paper. The authors also thank Dr. Navreet Kanwal Kaur Pannu for her expert technical assistance.

References

- Skitzki JJ, Repasky EA, Evans SS (2009) Hyperthermia as an immunotherapy strategy for cancer. *Curr Opin Investig Drugs*. 10: 550-558.
- Noessner E, Gastpar R, Milani V, Brandl A, Hutzler PJS, et al. (2002) Tumor-derived heat shock protein 70 peptide complexes are cross-presented by human dendritic cells. *J Immunol* 169: 5424-5432.
- Asea A, Kraeft SK, Kurt-Jones EA, Stevenson MA, Chen LB, et al. (2000) HSP70 stimulates cytokine production through a CD14-dependant pathway, demonstrating its dual role as a chaperone and cytokine. *Nat Med* 6: 435-442.
- Asea A, Rehli M, Kabingu E, Boch JA, Bare O, et al. (2002) Novel signal transduction pathway utilized by extracellular HSP70: role of toll-like receptor (TLR) 2 and TLR4. *J Biol Chem* 277: 15028-15034.
- Binder RJ, Harris ML, Ménoret A, Srivastava PK (2000) Saturation, competition, and specificity in interaction of heat shock proteins (hsp) gp96, hsp90, and hsp70 with CD11b+ cells. *J Immunol* 165: 2582-2587.
- Asea A (2008) Hsp70: a chaperokine. *Novartis Found Symp* 291: 173-179.
- Mambula SS, Calderwood SK (2006) Heat shock protein 70 is secreted from tumor cells by a nonclassical pathway involving lysosomal endosomes. *J Immunol* 177: 7849-7857.
- Bausero MA, Gastpar R, Multhoff G, Asea A (2005) Alternative mechanism by which IFN-gamma enhances tumor recognition: active release of heat shock protein 72. *J Immunol* 175: 2900-2912.
- Diagaradjane P, Shetty A, Wang JC, Elliott AM, Schwartz J, et al. (2008) Modulation of in vivo tumor radiation response via gold nanoshell-mediated vascular-focused hyperthermia: Characterizing an integrated antihypoxic and localized vascular disrupting targeting strategy. *Nano Lett* 8: 1492-1500.
- Dickson JA, Calderwood SK (1980) Temperature range and selective sensitivity of tumors to hyperthermia: a critical review. *Ann N Y Acad Sci* 335: 180-205.
- Mohrmann K, Gerez L, Oorschot V, Klumperman J, van der Sluijs P (2002) Rab4 function in membrane recycling from early endosomes depends on a membrane to cytoplasm cycle. *J Biol Chem* 277: 32029-32035.
- Mohrmann K, Leijendekker R, Gerez L, van Der Sluijs P (2002) rab4 regulates transport to the apical plasma membrane in Madin-Darby canine kidney cells. *J Biol Chem* 277: 10474-10481.
- Murshid A, Presley JF (2004) ER-to-Golgi transport and cytoskeletal interactions in animal cells. *Cell Mol Life Sci* 61: 133-145.
- Simons K, Ikonen E (1997) Functional rafts in cell membranes. *Nature* 387: 569-572.
- Asea A, Ara G, Teicher BA, Stevenson MA, Calderwood SK (2001) Effects of the flavonoid drug quercetin on the response of human prostate tumours to hyperthermia in vitro and in vivo. *Int J Hyperthermia* 17: 347-356.
- Asea A, Mallick R, Lechpammer S, Ara G, Teicher BA, et al. (2001) Cyclooxygenase inhibitors are potent sensitizers of prostate tumours to hyperthermia and radiation. *Int J Hyperthermia* 17: 401-414.
- Overgaard J (1981) Fractionated radiation and hyperthermia: Experimental and clinical studies. *Cancer* 48: 1116-1123.
- van der Zee J, Gonzalez Gonzalez D, van Rhooen GC, van Dijk JD, van Putten WL, et al. (2000) Comparison of radiotherapy alone with radiotherapy plus hyperthermia in locally advanced pelvic tumours: a prospective, randomised, multicentre trial. *Lancet* 355: 1119-1125.
- Harima Y, Nagata K, Harima K, Ostapenko VV, Tanaka Y, et al. (2001) A randomized clinical trial of radiation therapy versus thermoradiotherapy in stage IIIB cervical carcinoma. *Int J Hyperthermia* 17: 97-105.
- Jones EL, Oleson JR, Prosnitz LR, Samulski TV, Vujaskovic Z, et al. (2005) Randomized trial of hyperthermia and radiation for superficial tumors. *J Clin Oncol* 23: 3079-3085.
- Urano M, Kahn J, Majima H, Gerweck LE (1990) The cytotoxic effect of cis-diamminedichloroplatinum(II) on cultured Chinese hamster ovary cells at elevated temperatures: Arrhenius plot analysis. *Int J Hyperthermia* 6: 581-590.
- Majima H, Urano M, Sougawa M, Kahn J (1992) Radiation and thermal sensitivities of murine tumor (FSa-II) cells recurrent after a heavy irradiation. *Int J Radiat Oncol Biol Phys* 22: 1019-1028.
- Jones E, Alvarez Secord A, Prosnitz LR, Samulski TV, Oleson JR, et al. (2006) Intra-peritoneal cisplatin and whole abdomen hyperthermia for relapsed ovarian carcinoma. *Int J Hyperthermia*. 22: 161-172.
- Rietbroek RC, van de Vaart PJ, Haveman J, Blommaert FA, Geerdink A, et al. (1997) Hyperthermia enhances the cytotoxicity and platinum-DNA adduct formation of lobaplatin and oxaliplatin in cultured SW 1573 cells. *J Cancer Res Clin Oncol* 123: 6-12.
- de Wit R, van der Zee J, van der Burg ME, Kruit WH, Logmans A, et al. (1999) A phase I/II study of combined weekly systemic cisplatin and locoregional hyperthermia in patients with previously irradiated recurrent carcinoma of the uterine cervix. *Br J Cancer* 80: 1387-1391.
- Herman TS, Jochelson MS, Teicher BA, Scott PJ, Hansen J, et al. (1989) A phase I-II trial of cisplatin, hyperthermia and radiation in patients with locally advanced malignancies. *Int J Radiat Oncol Biol Phys* 17: 1273-1279.
- Westermann AM, Grosen EA, Katschinski DM, Jager D, Rietbroek R, et al. (2001) A pilot study of whole body hyperthermia and carboplatin in platinum-resistant ovarian cancer. *Eur J Cancer* 37: 1111-1117.
- Jones EL, Samulski TV, Dewhirst MW, Alvarez-Secord A, Berchuck A, et al. (2003) A pilot Phase II trial of concurrent radiotherapy, chemotherapy, and hyperthermia for locally advanced cervical carcinoma. *Cancer* 98: 277-2782.
- Westermann AM, Jones EL, Schem BC, van der Steen-Banasik EM, Koper P, et al. (2005) First results of triple-modality treatment combining radiotherapy, chemotherapy, and hyperthermia for the treatment of patients with stage IIB, III, and IVA cervical carcinoma. *Cancer* 104: 763-770.
- Srivastava PK (2005) Immunotherapy for human cancer using heat shock protein-peptide complexes. *Curr Oncol Rep* 7: 104-108.
- Srivastava PK (2000) Heat shock protein-based novel immunotherapies. *Drug News Perspect* 13: 517-522.
- Srivastava PK, Udono H, Blachere NE, Li Z (1994) Heat shock proteins transfer peptides during antigen processing and CTL priming. *Immunogenetics* 39: 93-98.
- Basu S, Binder RJ, Suto R, Anderson KM, Srivastava PK (2000) Necrotic but not apoptotic cell death releases heat shock proteins, which deliver a partial maturation signal to dendritic cells and activate the NF-kappa B pathway. *Int Immunol* 12: 1539-1546.
- Srivastava P (2002) Interaction of heat shock proteins with peptides and antigen presenting cells: chaperoning of the innate and adaptive immune responses. *Annu Rev Immunol* 20: 395-425.
- Panjwani NN, Popova L, Srivastava PK (2002) Heat shock proteins gp96 and hsp70 activate the release of nitric oxide by APCs. *J Immunol* 168: 2997-3003.
- Lehner T, Bergmeier LA, Wang Y, Tao L, Sing M, et al. (2000) Heat shock proteins generate beta-chemokines which function as innate adjuvants enhancing adaptive immunity. *Eur J Immunol* 30: 594-603.
- Asea A, Kabingu E, Stevenson MA, Calderwood SK (2000) HSP70 peptide-mimetic and peptide-negative preparations act as chaperokines. *Cell Stress Chaperones* 5: 425-431.
- Basu S, Suto R, Binder RJ, Srivastava PK (1998) Heat shock proteins as novel mediators of cytokine secretion by macrophages. *Cell Stress Chaperones* 3: 11-16.

39. Singh-Jasuja H, Toes RE, Spee P, Munz C, Hilf N, et al. (2000) Cross-presentation of glycoprotein 96-associated antigens on major histocompatibility complex class I molecules requires receptor-mediated endocytosis. *Journal of Experimental Medicine* 191: 1965-1974.
40. Ostberg JR, Gellin C, Patel R, Repasky EA (2001) Regulatory potential of fever-range whole body hyperthermia on Langerhans cells and lymphocytes in an antigen-dependent cellular immune response. *J Immunol* 167: 2666-2670.
41. Evans SS, Wang WC, Bain MD, Burd R, Ostberg JR, et al. (2001) Fever-range hyperthermia dynamically regulates lymphocyte delivery to high endothelial venules. *Blood* 97: 2727-2733.
42. Rapoport TA, Matlack KE, Plath K, Misselwitz B, Staack O (1999) Posttranslational protein translocation across the membrane of the endoplasmic reticulum. *Biol Chem* 380: 1143-1150.
43. Ferrari D, Pizzirani C, Adinolfi E, Lemoli RM, Curti A, et al. (2006) The P2X7 receptor: a key player in IL-1 processing and release. *J Immunol* 176: 3877-3883.
44. Wewers MD (2004) IL-1beta: an endosomal exit. *Proc Natl Acad Sci USA* 101: 10241-10242.
45. Gastpar R, Gehrman M, Bausero MA, Asea A, Gross C, et al. (2005) Heat shock protein 70 surface-positive tumor exosomes stimulate migratory and cytolytic activity of natural killer cells. *Cancer Res* 65: 5238-5247.
46. Mambula SS, Calderwood SK (2006) Heat induced release of Hsp70 from prostate carcinoma cells involves both active secretion and passive release from necrotic cells. *Int J Hyperthermia* 22: 575-585.
47. Mambula SS, Stevenson MA, Ogawa K, Calderwood SK (2007) Mechanisms for Hsp70 secretion: crossing membranes without a leader. *Methods* 43: 168-175.
48. Srivastava PK (2003) Hypothesis: controlled necrosis as a tool for immunotherapy of human cancer. *Cancer Immun* 3: 4.
49. Daniels GA, Sanchez-Perez L, Diaz RM, Kottke T, Thompson J, et al. (2004) A simple method to cure established tumors by inflammatory killing of normal cells. *Nat Biotechnol* 22: 1125-1132.
50. Ganley IG, Carroll K, Bittova L, Pfeffer S (2004) Rab9 GTPase regulates late endosome size and requires effector interaction for its stability. *Mol Biol Cell* 15: 5420-5430.
51. Yeaman C, Grindstaff KK, Wright JR, Nelson WJ (2001) Sec6/8 complexes on trans-Golgi network and plasma membrane regulate late stages of exocytosis in mammalian cells. *J Cell Biol* 155: 593-604.
52. Matern HT, Yeaman C, Nelson WJ, Scheller RH (2001) The Sec6/8 complex in mammalian cells: characterization of mammalian Sec3, subunit interactions, and expression of subunits in polarized cells. *Proc Natl Acad Sci U S A* 98: 9648-9653.
53. Ang AL, Folsch H, Koivisto UM, Pypaert M, Mellman I (2003) The Rab8 GTPase selectively regulates AP-1B-dependent basolateral transport in polarized Madin-Darby canine kidney cells. *J Cell Biol* 163: 339-350.
54. Wunderlich W, Fialka I, Teis D, Alpi A, Pfeifer A, et al. (2001) A novel 14-kilodalton protein interacts with the mitogen-activated protein kinase scaffold mp1 on a late endosomal/lysosomal compartment. *J Cell Biol* 152: 765-776.
55. Teis D, Wunderlich W, Huber LA (2002) Localization of the MP1-MAPK scaffold complex to endosomes is mediated by p14 and required for signal transduction. *Dev Cell* 3: 803-814.
56. Cuervo AM, Dice JF (1996) A receptor for the selective uptake and degradation of proteins by lysosomes. *Science* 273: 501-503.
57. Cuervo AM, Hu W, Lim B, Dice JF (1998) I kappaB is a substrate for a selective pathway of lysosomal proteolysis. *Mol Biol Cell* 9: 1995-2010.
58. Oestreich AJ, Aboian M, Lee J, Azmi I, Payne J, et al. (2007) Characterization of multiple multivesicular body sorting determinants within Sna3: a role for the ubiquitin ligase Rsp5. *Mol Biol Cell* 18: 707-720.
59. Asea A (2003) Chaperone-induced signal transduction pathways. *Exerc Immunol Rev* 9: 25-33.
60. Asea A (2004) Exogenous Hsp70: principles and application of the chaperone activity of Hsp70. In: Henderson B, Pockley AG (Eds.) *The Extracellular Biology of Molecular Chaperones*. Cambridge University Press, London.
61. Singh-Jasuja H, Scherer HU, Hilf N, Arnold-Schild D, Rammensee HG, et al. (2000) The heat shock protein gp96 induces maturation of dendritic cells and down-regulation of its receptor. *Eur J Immunol* 30: 2211-2215.
62. Binder RJ, Anderson KM, Basu S, Srivastava PK (2000) Cutting edge: heat shock protein gp96 induces maturation and migration of CD11c+ cells in vivo. *J Immunol* 165: 6029-6035.
63. Udono H, Srivastava PK (1993) Heat shock protein 70-associated peptides elicit specific cancer immunity. *J Exp Med* 178: 1391-1396.
64. Testori A, Richards J, Whitman E, Mann GB, Lutzky J, et al. (2008) Phase III comparison of vitespen, an autologous tumor-derived heat shock protein gp96 peptide complex vaccine, with physician's choice of treatment for stage IV melanoma: the C-100-21 Study Group. *J Clin Oncol* 26: 955-962.
65. Jonasch E, Wood C, Tamboli P, Pagliaro LC, Tu SM, et al. (2008) Vaccination of metastatic renal cell carcinoma patients with autologous tumour-derived vitespen vaccine: clinical findings. *Br J Cancer* 98: 1336-1341.
66. Maki RG, Livingston PO, Lewis JJ, Janetzki S, Klimstra D, et al. (2007) A phase I pilot study of autologous heat shock protein vaccine HSPPC-96 in patients with resected pancreatic adenocarcinoma. *Dig Dis Sci* 52: 1964-1972.
67. van der Zee J (2002) Heating the patient: A promising approach?. *Ann Oncol* 13: 1173-1184.
68. Reinhold HS, Endrich B (1986) Tumour microcirculation as a target for hyperthermia. *Int J Hyperthermia* 2: 111-137.
69. Corry PM, Robinson S, Getz S (1977) Hyperthermic effects on DNA repair mechanisms. *Radiology* 123: 475-482.
70. Wong RS, Dynlacht JR, Cedervall B, Dewey WC (1995) Analysis by pulsed-field gel electrophoresis of DNA double-strand breaks induced by heat and/or X-irradiation in bulk and replicating DNA of CHO cells. *Int J Radiat Biol* 68: 141-152.
71. Seno JD, Dynlacht JR (2004) Intracellular redistribution and modification of proteins of the Mre11/Rad50/Nbs1 DNA repair complex following irradiation and heat-shock. *J Cell Physiol* 199: 157-170.
72. Thompson LH, Schild D (2002) Recombinational DNA repair and human disease. *Mutat Res* 509: 49-78.
73. Song CW, Shakil A, Griffin RJ, Okajima K (1997) Improvement of tumor oxygenation status by mild temperature hyperthermia alone or in combination with carbogen. *Semin Oncol* 24: 626-632.
74. Kampinga HH, Dikomey E (2001) Hyperthermic radiosensitization: Mode of action and clinical relevance. *Int J Radiat Biol* 77: 399-408.
75. Marino C, Cividalli A (1992) Combined radiation and hyperthermia: Effects of the number of heat fractions and their interval on normal and tumour tissues. *Int J Hyperthermia* 8: 771-781.